

SCIENTIFIC REPORTS



OPEN

MicroRNA-98 negatively regulates myocardial infarction-induced apoptosis by down-regulating Fas and caspase-3

Chuan Sun¹, Huibin Liu¹, Jing Guo¹, Yang Yu¹, Di Yang¹, Fang He¹ & Zhimin Du^{1,2}

Acute myocardial infarction (MI) is the leading cause of sudden death worldwide. MicroRNAs (miRs) is a novel class of regulators of cardiovascular diseases such as MI. This study aimed to explore the role of miR-98 in MI and its underlying mechanisms. We found that miR-98 was downregulated both in infarcted and ischemic myocardium of MI mice as well as H₂O₂-treated neonatal rat ventricular myocytes (NRVCs). miR-98 overexpression remarkably increased cell viability and inhibited apoptosis of H₂O₂-treated NRVCs. Meanwhile, overexpression of miR-98 reversed H₂O₂-induced Bcl-2 downregulation and Bax elevation and significantly reduced JC-1 monomeric cells. Meanwhile, miR-98 overexpression attenuated the upregulation of Fas and caspase-3 in H₂O₂-treated cardiomyocytes at the mRNA and protein levels. Dual-luciferase reporter assay showed that miR-98 directly targeted to Fas 3'-UTR. Furthermore, MI mice injected with miR-98-agomir had a significant reduction of apoptotic cells, the serum LDH levels, myocardial caspase-3 activity, Fas and caspase-3 expression in heart tissues. Administration of miR-98-agomir also showed decreased infarct size and improved cardiac function. Collectively, miR-98 is downregulated in the MI heart and NRVCs in response to H₂O₂ stress, and miR-98 overexpression protects cardiomyocytes against apoptosis. Anti-apoptotic effects of miR-98 are associated with regulation of Fas/Caspase-3 apoptotic signal pathway.

Acute myocardial infarction (AMI), resulting from coronary artery occlusion, is the most common causes of cardiovascular morbidity and mortality worldwide¹. Apoptosis, which is triggered by an imbalance between pro- and anti-apoptotic factors, is frequently detected in ischemic heart tissue². Cardiomyocyte apoptotic death in the border area close to myocardial infarcted area leads to cardiomyocyte loss, aggravates cardiac dysfunction and even causes heart failure and mortality^{3,4}. Therefore, targeting inhibition of cardiomyocytes apoptosis during early stage of MI is critical for reducing infarct size and promoting cardiac repair, which is a key approach for treating ischemic heart disease. However, the molecular components regulating AMI-induced apoptosis in cardiomyocytes remain poorly understood.

MicroRNAs (miRNAs) are a group of small, endogenous and non-coding RNA molecules, with about 22 nucleotides in length, which has been shown to post-transcriptionally regulate the expression of target genes, leading to the destruction and degeneration of mRNAs⁵. Clinical trials and animal experiments indicate that miRNAs are potential biomarkers and therapeutic targets for cardiac ischemia^{6,7}. Moreover, several miRNAs are implicated in playing regulatory roles in cardiomyocytes apoptosis. Recent studies elucidate that miR-21, -24, -133, -210, -494 and -499 prevent myocytes against ischemia/reperfusion-induced apoptosis, while miR-1, -29, -195, -199a, -497 and -320 promote apoptosis⁸⁻¹⁰. Our previous study has also shown that combination of miR-21 and miR-146a has a greater protective effect against cardiac ischemia/hypoxia-induced apoptosis¹¹.

MiR-98 is one of the members of the let-7 miRNA family, which is first discovered to control the developmental timing of cell differentiation and proliferation in *C. elegans*^{12,13}. Recently, altered miR-98 expression has been found in several carcinomas¹⁴. Therefore, let-7/miR-98 miRNAs are considered as an oncomir family crucial

¹Institute of Clinical Pharmacy, the Second Affiliated Hospital of Harbin Medical University (The University Key Laboratory of Drug Research, Heilongjiang Province), Harbin, 150086, China. ²Department of Clinical Pharmacology, College of Pharmacy, Harbin Medical University, Harbin, 150086, China. Chuan Sun and Huibin Liu contributed equally to this work. Correspondence and requests for materials should be addressed to Z.D. (email: dzm1956@126.com)

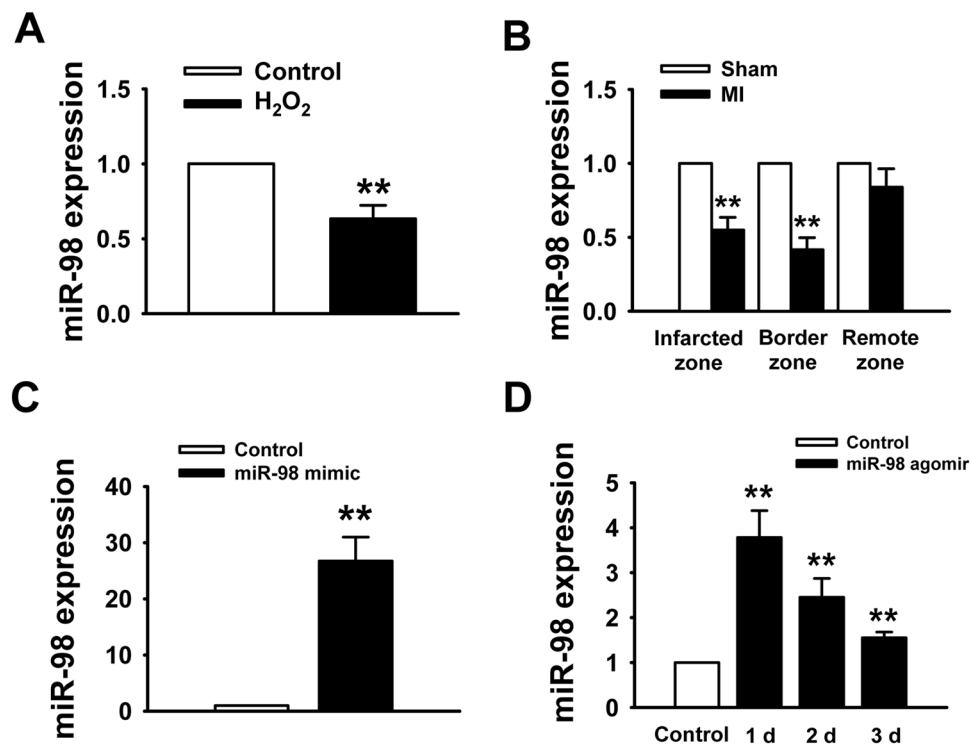


Figure 1. MiR-98 is downregulated in MI mice model and H_2O_2 -treated NRVCs. **(A)** Real-time PCR data showed the downregulation of miR-98 expression in NRVCs treated with $100\ \mu M$ H_2O_2 for 4 h. $n = 6$. **(B)** miR-98 is decreased in the infarcted and border zones of MI mice compared with sham mice. $n = 3$. **(C)** miR-98 expression level in NRVCs after miR-98 mimic transfection. $n = 6$. **(D)** miR-98 expression level in rat ventricles after administration with miR-98 agomir. $n = 3$. ** $P < 0.01$ vs. Control or Sham.

in regulating cell cycle and apoptosis¹⁵. Moreover, miR-98 has been reported to be a sensitive marker of renal ischemic injury¹⁶ and protect endothelial cells against hypoxia/reoxygenation induced-apoptosis by targeting caspase-3¹⁷. In addition, miR-98 was verified to target Fas directly and regulated Fas-mediated apoptosis in HeLa cells¹⁸. However, the functional roles of miR-98 in cardiomyocytes apoptosis during early stage of MI have not previously been investigated.

In the current study, we employed a mouse MI model and H_2O_2 -induced cardiomyocyte injury model to investigate whether miR-98 had a protective effect against MI-induced cardiomyocytes apoptosis and myocardial dysfunction. Our findings suggest that miR-98 may provide a potential novel therapeutic approach for the treatment of ischemic heart disease.

Results

MiR-98 is downregulated in response to myocardial ischemic injury. Firstly, the expression of miR-98 was detected in H_2O_2 -treated cardiomyocytes and postinfarct cardiac tissues. As our previous study¹⁰ reported that H_2O_2 reduced cardiomyocyte viability in a concentration and time-dependent manner, we chose $100\ \mu M$ H_2O_2 treated NRVCs for 4 h as a cardiomyocyte injury model in this study. As shown in Fig. 1A, compared with control group, miR-98 expression was significantly decreased by exposure to $100\ \mu M$ H_2O_2 in NRVCs. Meanwhile, we also examined the expression of miR-98 in heart tissues after MI for 3 days. To determine the change of miR-98 in the different areas of infarcted hearts, miRNAs were isolated from infarcted zone, border zone and remote zone. Real-time PCR analysis revealed that the expression of miR-98 in the infarcted and border zones of rat hearts at 3 days after MI was much lower than that in sham-operated animals (Fig. 1B).

Then, we overexpressed miR-98 in NRVCs by miR-98 mimic transfection and in mice hearts by miR-98 agomir injection. We validated the miR-98 level using Real-time PCR, and found that miR-98 level was significantly higher in miR-98 mimic transfection group than that in non-transfection group (Fig. 1C). As shown in Fig. 1D, 1, 2 and 3 days after injection of miR-98 agomir using our delivery method, miR-98 expression was markedly increased in the heart tissue.

MiR-98 overexpression prevented H_2O_2 -induced cardiomyocyte apoptosis. Based on the above results, we subsequently aimed to evaluate the effects of miR-98 overexpression on cell apoptosis. Cells subjected to $100\ \mu M$ H_2O_2 for 4 h showed markedly decreased viability by MTT assay (Fig. 2A). In contrast, compared with miRNA negative control (NC) transfection group, miR-98 overexpression by transfecting with miR-98 mimic significantly increased the cell viability of NRVCs treated with H_2O_2 (Fig. 2A). Furthermore, it was observed that the number of TUNEL-positive cells was significantly increased in H_2O_2 group, which was diminished by miR-98

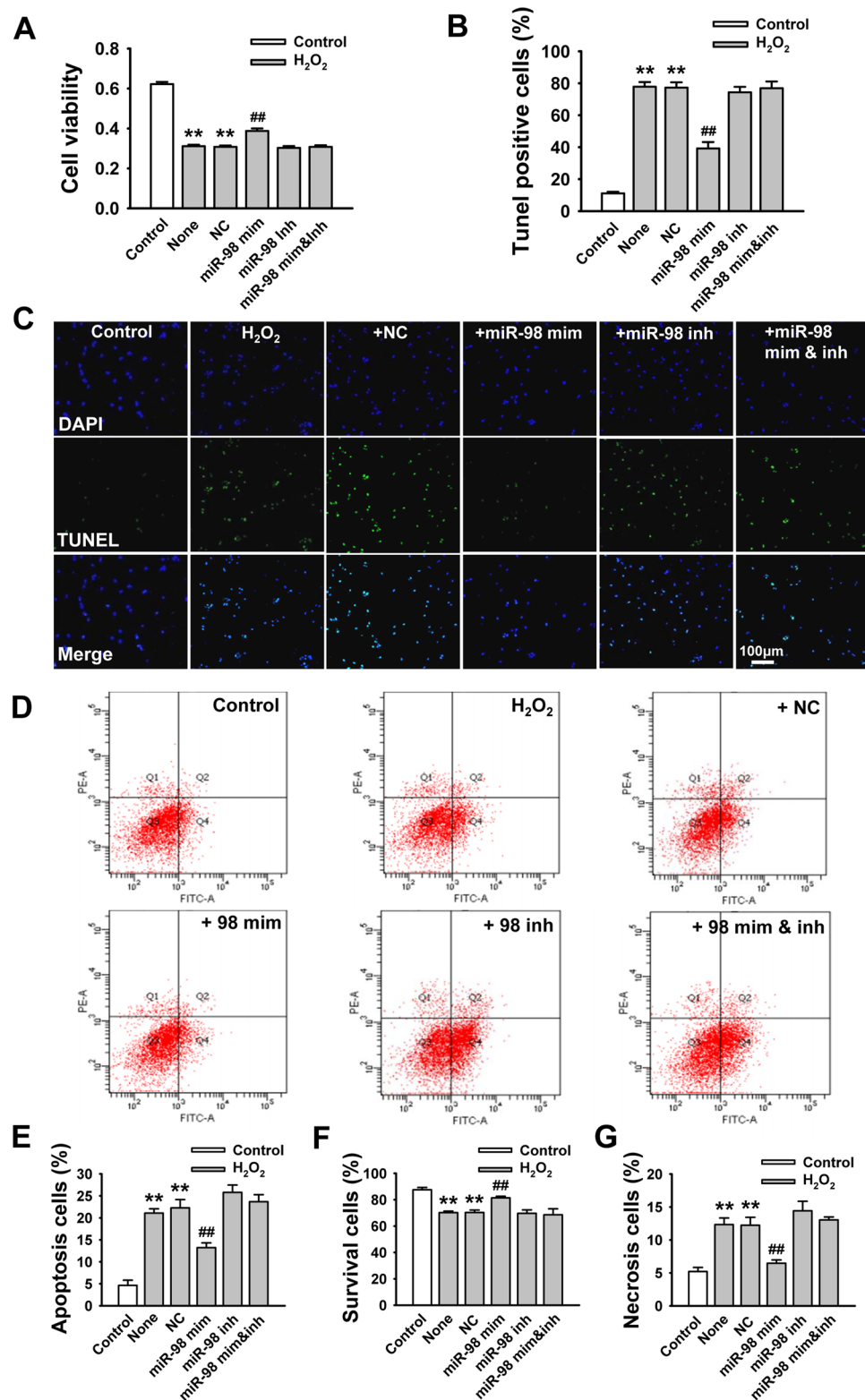


Figure 2. Overexpression of miR-98 prevents cardiomyocyte apoptosis in response to H₂O₂. NRVCs were transfected with NC (negative control), miR-98 mimic (miR-98 mim), miR-98 inhibitor (miR-98 inh), and miR-98 mimic + inhibitor (miR-98 mim&inh) and then treated with H₂O₂ (100 μM) for 4 h. (A) MTT assay suggested that miR-98 mimic restored cell viability of NRVCs treated with 100 μM H₂O₂ for 4 h. n = 8. (B) Statistical results of TUNEL-positive cells per field indicated that miR-98 mimic suppressed H₂O₂ treatment-induced cell apoptosis. n = 6. (C) Representative images of TUNEL staining of NRVCs for DNA defragmentation showing the apoptotic cells (nucleus stained in blue with DAPI and apoptotic cells stained in green). (D) The representative images of flow cytometry using Annexin V-FITC and PI staining. (E)-(G) Statistical analysis of apoptotic, survival and necrosis ratio of the flow cytometry data. n = 4; **P < 0.01 versus control; ##P < 0.01 versus H₂O₂ + NC cells.

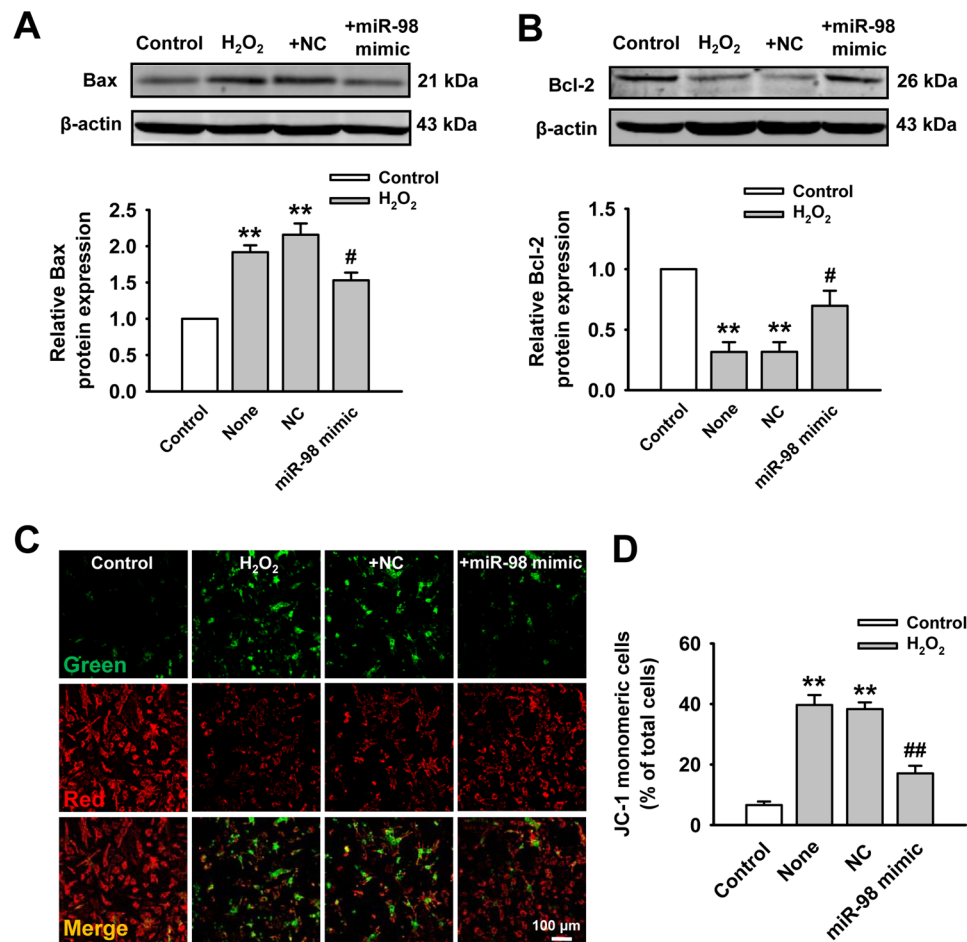


Figure 3. Effect of miR-98 on Bax and Bcl-2 expression and mitochondrial membrane potential ($\Delta\psi_m$). (A) miR-98 overexpression reduced H₂O₂-induced elevation of Bax expression. Cropped blots are shown. Full-length blots are presented in Supplementary Fig. S1. n = 6. (B) Bcl-2 expression was suppressed by H₂O₂ but upregulated by miR-98. Cropped blots are shown. Full-length blots are presented in Supplementary Fig. S2. n = 6. (C) Upper panels show representative fluorescent images of JC-1 monomeric mitochondria showing green fluorescence and JC-1 aggregated mitochondria from Control, H₂O₂, H₂O₂ + NC and H₂O₂ + miR-98 mimic groups. (D) Overexpression of miR-98 reduced H₂O₂-induced JC-1 monomeric mitochondria. n = 5. ***P* < 0.01 versus control; #*P* < 0.05, ##*P* < 0.01 versus H₂O₂ + NC cells.

mimic but not by NC or miR-98 inhibitor (Fig. 2B and C). In addition, flow cytometry was utilized to validate the protective role of miR-98 in H₂O₂-induced cardiomyocyte apoptosis. We found that the apoptosis percentage was increased by H₂O₂ treatment, which was significantly diminished by miR-98 mimic (Figure 2D and E).

Furthermore, the effect of miR-98 mimic on H₂O₂-induced cell apoptosis was abolished by co-transfection with miR-98 inhibitor (Fig. 2D and E). Moreover, overexpression of miR-98 also increased cell viability and prevented cell necrosis in H₂O₂-treated NRVCs (Fig. 2F and G). Taken together, these results proved that miR-98 overexpression prevented H₂O₂-induced cardiomyocyte apoptosis and promoted cell survival.

MiR-98 overexpression regulates apoptosis-related proteins and mitochondrial membrane potential. Since miR-98 promoted cell survival and prevented cardiomyocyte apoptosis, we further investigated its role in regulating the expression of apoptosis-related proteins and mitochondrial membrane potential ($\Delta\psi_m$). Bax is pro-apoptotic protein which is absent/or very less in normal rat myocardium. As shown in Fig. 3A, exposure to H₂O₂ increased the Bax expression. However, miR-98 overexpression induced a sharp decrease of Bax expression in NRVCs compared with NC group (Fig. 3A). Antiapoptotic protein Bcl-2 was expressed in healthy control NRVCs. But exposure of NRVCs to H₂O₂ showed lower expression level of Bcl-2 than those in control NRVCs. Also, Bcl-2 expression was elevated in NRVCs after miR-98 overexpression (Fig. 3B). The corresponding densitometry analysis exhibited similar as the above descriptions (Fig. 3A and B).

Mitochondrial damage was determined using a mitochondrial membrane potential kit. The increase in the number of JC-1 monomeric cells (green) reflected the loss of $\Delta\psi_m$. Compared with control cells, the number of JC-1 monomeric cells was remarkably increased in H₂O₂-stimulated cells. However, H₂O₂-induced increase in monomeric form cells was reduced by miR-98 overexpression (Fig. 3C and D).

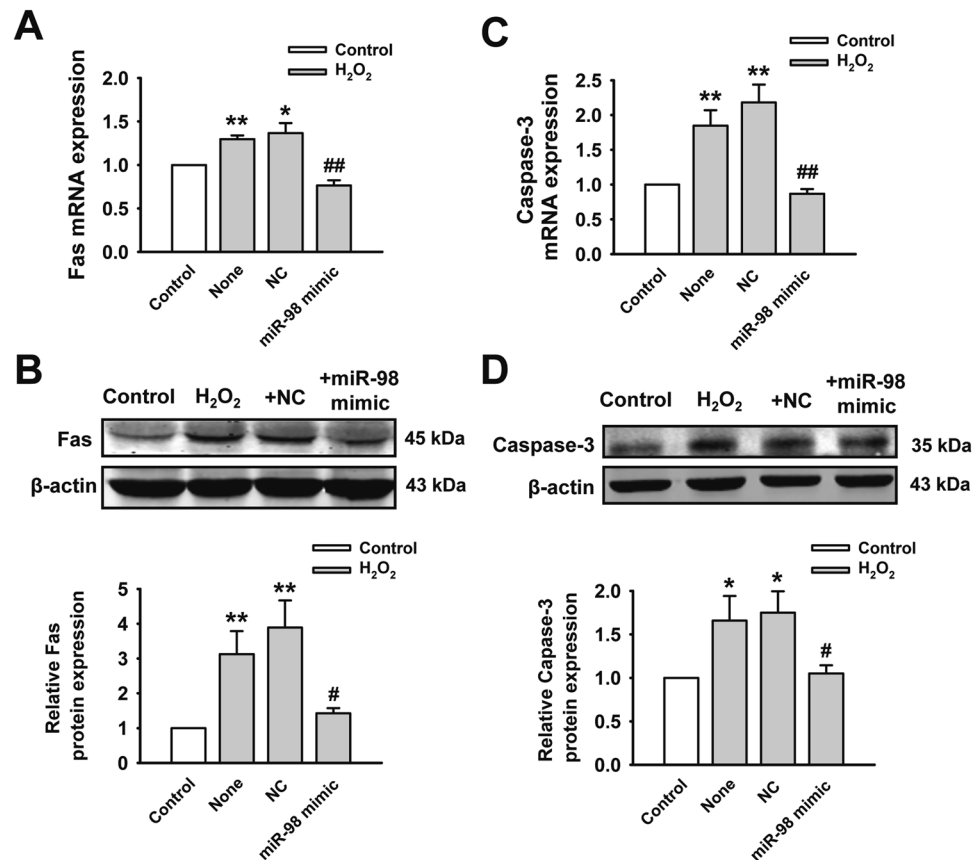


Figure 4. MiR-98 overexpression inhibits the expression of Fas and caspase-3. (A) and (B) MiR-98 overexpression significantly prevented upregulation of Fas mRNA and protein level in H₂O₂-treated NRVCs. Cropped blots are shown. Full-length blots are presented in Supplementary Fig. S3. n = 5. (C) and (D) The mRNA and protein expression of caspase-3 were also remarkably elevated by H₂O₂ but reduced by miR-98 overexpression. Cropped blots are shown. Full-length blots are presented in Supplementary Fig. S4. n = 6. **P* < 0.05, ***P* < 0.01 versus control; #*P* < 0.05, ##*P* < 0.01 versus H₂O₂ + NC cells.

MiR-98 overexpression suppresses H₂O₂-induced upregulation of Fas and caspase-3 in cardiomyocytes. We next aimed to explore the underlying mechanism that miR-98 inhibited H₂O₂-induced apoptosis. As Fas and caspase-3 were proved to be the target genes of miR-98^{17,18}, we further verified the expression of Fas and caspase-3 in the presence of miR-98 overexpression. As shown in Fig. 4A, compared with control group, Fas mRNA expression was significantly upregulated in the H₂O₂-treated NRVCs, which could be reversed by miR-98 overexpression. Furthermore, it is worth noting that the protein expression of Fas was markedly higher under H₂O₂ conditions than those in H₂O₂-free group. MiR-98 overexpression led to the decreased Fas protein expression in posttranscriptional level (Fig. 4B), further indicating that Fas was the target gene of miR-98. Meanwhile, miR-98 overexpression also reduced the upregulation of caspase-3 mRNA induced by H₂O₂ (Fig. 4C). The protein level of caspase-3 after miR-98 mimic transfection showed the similar trend with the mRNA level (Fig. 4D). Consequently, miR-98 could reverse the H₂O₂ induced elevation of Fas and caspase-3, and thus provide protections against ischemia-induced cardiomyocyte apoptosis.

MiR-98 directly targets at the 3'-UTR of Fas. Fas and caspase-3 were identified to be the target genes of miR-98 in humans^{17,18} and the predicted site in caspase-3 3'-UTR showed a good conservative character among different species¹⁷. Due to the non-homology of Fas in different species, we used computational methods to search for the potential targets of miR-98 in rats and constructed luciferase reporter plasmids containing the 3'-UTR of Fas. The binding sites of miR-98 in the 3'-UTR of wild-type Fas mRNA were displayed, but mutant mRNA had few binding sites (Fig. 5A). We then transfected HEK293T cells with the luciferase vector containing a wild-type or mutant miR-98 response element. We cotransfected these cells with NC or miR-98 mimic and measured luciferase activity. miR-98 overexpression significantly inhibited luciferase activity in the wild-type group, demonstrating that miR-98 could target at 3'-UTR of Fas (Fig. 5B). However, miR-98 failed to affect the luciferase activity elicited by the construct carrying the Fas 3'-UTR with the mutant miR-98-binding site (Fig. 5C). Therefore, Fas was proved to be the target gene of miR-98.

Effect of miR-98 overexpression on ischemia-induced cardiomyocyte apoptosis. We then tried to clarify whether antiapoptotic effects of miR-98 on cultured cells under H₂O₂ conditions also exist under in

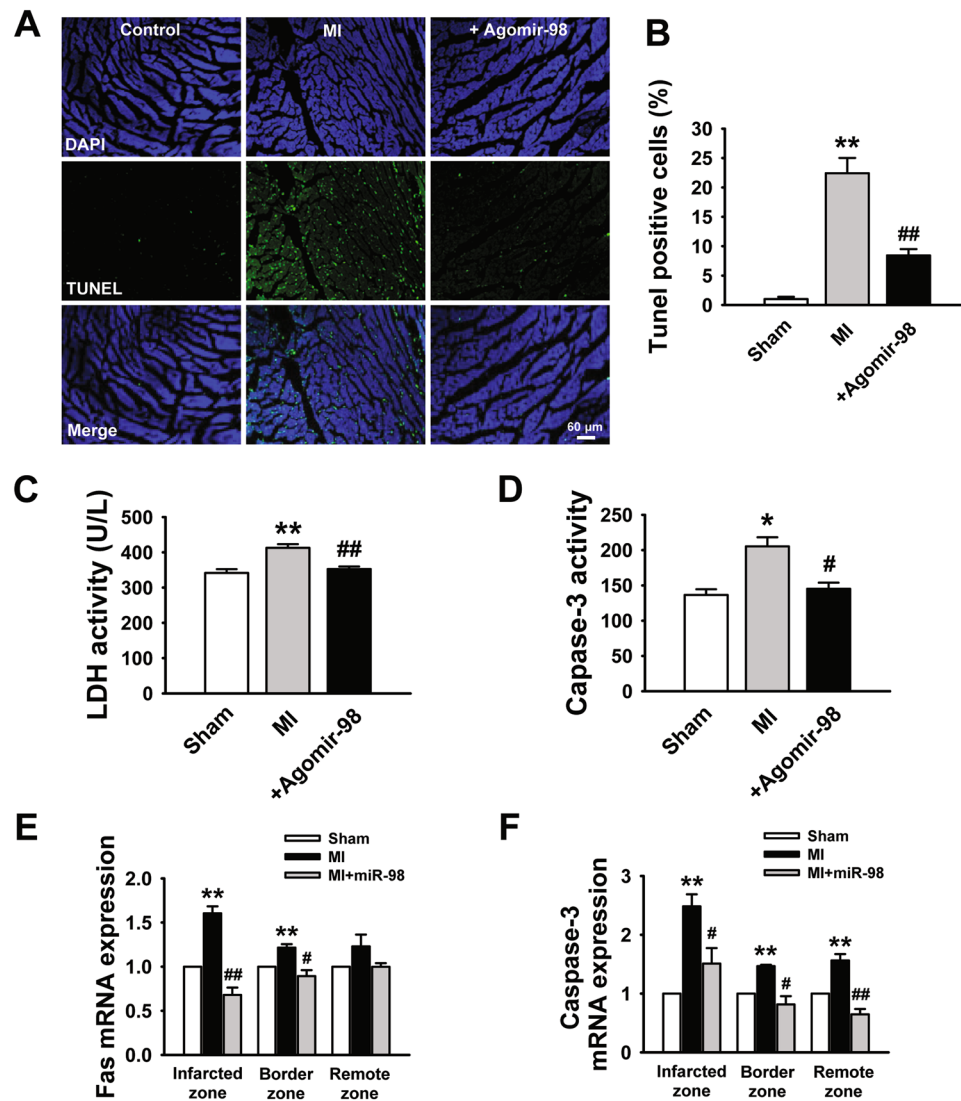


Figure 6. miR-98 protected cardiomyocytes against ischemia-induced apoptosis in a mouse MI model. **(A)** Effects of miR-98 agomir on cardiac apoptosis were evaluated by TUNEL staining. **(B)** The percentage of TUNEL-positive cell in different groups. $n = 6$. **(C)** Serum lactate dehydrogenase (LDH) activity is increased in MI mice and restored by miR-98 agomir administration. $n = 6$. **(D)** Caspase-3 activity is promoted in MI mice and reversed by miR-98 agomir. $n = 5$. **(E)** MiR-98 significantly prevented upregulation of Fas mRNA level in the infarcted and border zones of MI mice. $n = 5$. **(F)** MiR-98 suppressed the elevation of caspase-3 mRNA level in the infarcted, border and remote zones of MI mice. $n = 5$. * $P < 0.05$, ** $P < 0.01$ versus sham group; # $P < 0.05$, ## $P < 0.01$ versus MI group.

is extrinsic pathway, which concerns membrane-bound death receptors, such as Fas/Fas-L²³. We investigated whether the two apoptosis pathways were involved in the miR-98-mediated cardioprotection at the same time. Firstly, to investigate the effects of miR-98 on mitochondrial protection, we analyzed the expression of Bcl-2 and Bax and the mitochondrial membrane potential ($\Delta\psi_m$). Bcl-2 could prevent the release of cytochrome C from the mitochondria to the cytoplasm, and thus inhibit cell apoptosis²⁴. On the contrary, Bax could antagonize the function of Bcl-2 and therefore accelerate cell apoptosis²⁴. The intrinsic pathway relies on anti-apoptotic Bcl-2 and pro-apoptotic Bax proteins at mitochondria to sense stress, signal and execute apoptosis of the cell^{25,26}. The current results showed that overexpression of miR-98 reversed the reduction in Bcl-2 expression caused by acute ischemia, suggesting that Bcl-2 is involved in miR-98-induced cardioprotection. Meanwhile, miR-98 reduced the activation of Bax. A reduction in the $\Delta\psi_m$ is regarded as a hallmark of the early apoptotic period. The results show that the exposure of NRVCs to H_2O_2 caused a significant increase of JC-1 monomeric cells relative to that of the control group. By contrast, the number of JC-1 monomeric cells was markedly reduced in NRVCs overexpressed miR-98. Therefore, we have demonstrated for the first time that miR-98 protects against H_2O_2 -induced mitochondrial dysfunction in NRVCs.

Another mechanism of apoptosis in MI model is via signaling by death receptor members, such as Fas/Fas-L^{22,25,27}. Fas receptor mediated apoptosis has been reported in experimental myocardial infarction and in chronic heart

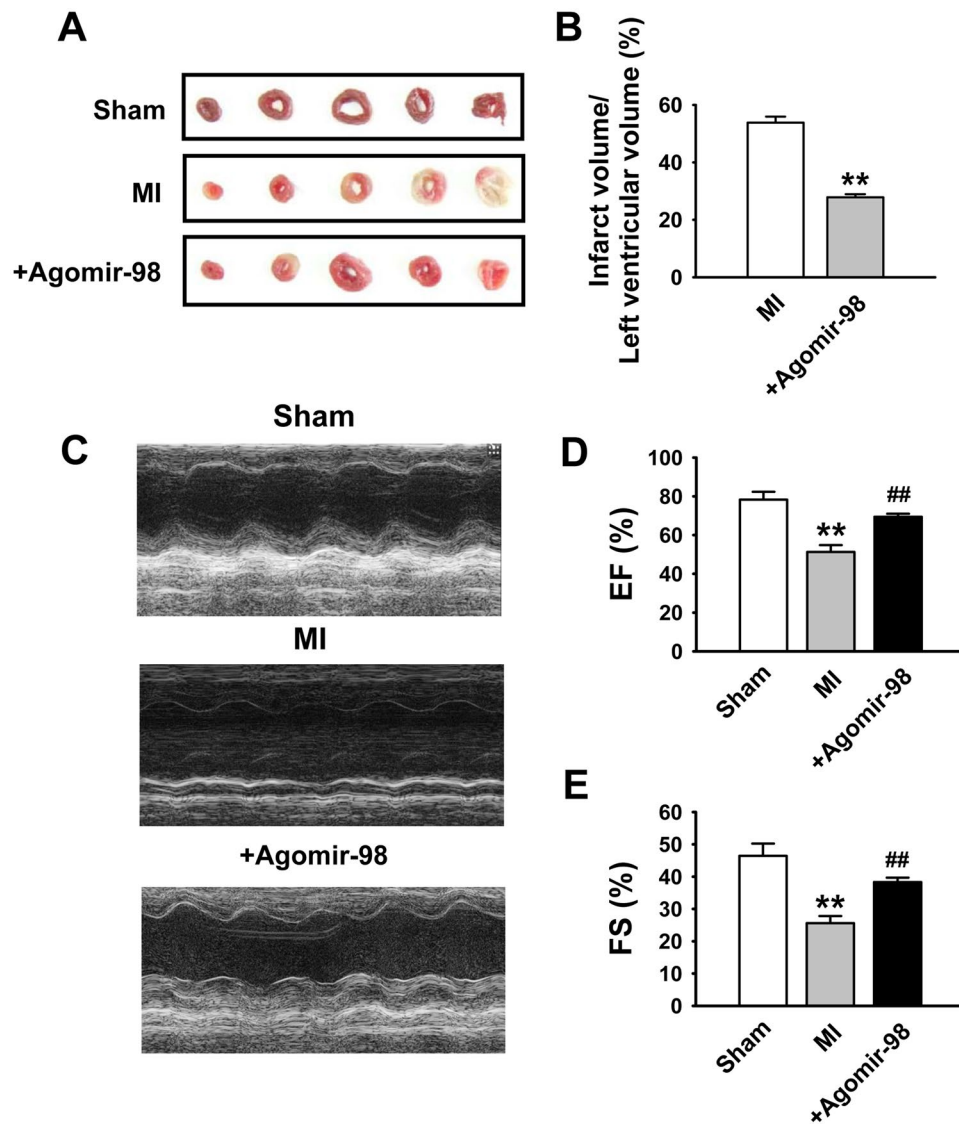


Figure 7. Reduction of infarct size and improvement of cardiac function by miR-98 in MI mice. (A) Representative images showing infarct areas in cross section slices. (B) Statistical analysis of IA/LV ratio. IA: infarct area, LV: left ventricles. $n = 3$. ** $P < 0.01$ versus MI group. (C) Representative photographs of heart function. (D) Ejection fractions (EF) and (E) Fractional shortening (FS). $n = 6$. ** $P < 0.01$ versus sham group; ## $P < 0.01$ versus MI group.

failure^{27,28}. Fas activation-induced cardiomyocytes apoptosis is also a critical mediator of MI²⁸. Enhanced expression of Fas-receptor may result in increasing response to myocardial injury, causing increased apoptosis. The present results showed that the expression of Fas was dramatically upregulated in the infarcted myocardium, the results are in accord with the previous study²⁸. At the same time, miR-98 significantly reversed the expression of Fas protein. Sequential activation of caspases plays a central role in the execution-phase of cell apoptosis. In general, the pro-apoptotic members of caspases-8 were looked as the initiators of apoptosis and caspase-3 was the executioners of apoptosis²⁹. Caspase-3 has been confirmed as a dominant executor in the Fas death pathway, which results in DNA degradation and apoptosis³⁰. Thus inhibition of the activity or function of caspase-3 may depress apoptosis³¹. Western blot showed that the expression caspase-3 was significantly decreased by miR-98. In addition, knockdown of Fas has been shown can significantly reduce Bax expression and increase Bcl-2 expression, which means the correlation between canonical apoptotic pathway and Fas/FasL pathway³². Therefore, we speculated that miR-98 simultaneously modulated of the intrinsic and extrinsic pathways of myocardial apoptosis in MI. However, the mechanism by which miR-98 reduced the apoptosis of cardiomyocytes through targeting Fas/Caspase-3 and simultaneously regulating mitochondrial apoptotic pathway remains to be elucidated.

In total, the present study demonstrates that miR-98 suppresses the apoptosis of cardiomyocytes, reduces the MI size, and improves the cardiac function. The cardioprotective effect of miR-98 was achieved by regulating Fas/Caspase-3 apoptotic signal pathway. This reveals that overexpression of miR-98 during the infarct period might be a useful approach for heart protection.

Methods

Animals. Healthy adult male Kunming mice (25–30g) used in the present study were kept under standard animal room conditions (temperature, $23 \pm 1^\circ\text{C}$; humidity, $55 \pm 5\%$) with food and water ad libitum for 1 week before the experiments. The study was approved by the Animal Care and Use Committee of Harbin Medical University. All experimental procedures were performed in accordance with the Guide for the Care and Use of Laboratory Animals, published by the US National Institutes of Health (NIH Publication, 8th Edition, 2011).

MI Model and Administration of miR-98 agomir. The miR-98 agomirs (Ribo-bio, Guangzhou, China) are double-stranded RNA analogues identical to the mature mmu-miR-98-5p (5'-UGAGGUAGUAAGUUGUAUUGUU-3'). The construct was chemically modified and conjugated with cholesterol moiety for in vivo applications with long-lasting stability and enhanced target specificity and affinity. Before surgery, mice were anesthetized with 2, 2, 2-Tribromoethanol (20 mg/kg) and ventilated. The chest was opened via the fourth intercostal space. The ascending aortic artery and the main pulmonary artery were clamped; then, miR-98 agomir ($200 \text{ nmol}\cdot\text{kg}^{-1}$ at the volume of $80 \mu\text{L}$) was injected into the left ventricular cavity through the tip of the heart with a 30-gauge syringe. The arteries were occluded for 10 seconds after injection. Mice in sham and MI groups underwent the same procedures but received $80 \mu\text{L}$ saline. Then MI was induced by ligation of the left anterior-descending (LAD) artery as described previously¹⁹. In brief, the standard limb lead ECG was continuously recorded on a recorder (BL-420, Taimeng, Chengdu, China). The heart was exposed through a left thoracotomy in the fourth intercostal space and the LAD artery was then ligated with 8–0 sutures was then looped around the LAD coronary artery. Sham-operated mice underwent an identical procedure except that the suture was passed around the vessel without LAD occlusion.

Measurement of infarct size. Three days after MI, the hearts were harvested and infarct size was measured by TTC (triphenyltetrazolium chloride, Sigma-Aldrich) staining as described previously^{17,33}. After washing out remaining blood and trimming out the right ventricle, the left ventricle was cut into 2-mm thick slices and stained with 1% TTC at 37°C for 20 minutes, and the infarct area was stainless while the live area turned red. The infarct area were calculated using Image ProPlus 5.0 software (Media Cybernetics, Wokingham, UK). For further study, the tissues in ischemic area of the hearts were collected and stored at -80°C .

Echocardiographic measurements. Three days after MI, cardiac function was examined by transthoracic echocardiography with an ultrasound machine (Panoview β 1500, Cold Spring Biotech, Taiwan, China) equipped with a 30-MHz phased-array transducer. M-mode tracings were used to measure percentage of ejection fraction (EF%) and fractional shortening (FS%) as described previously¹¹.

Neonatal rat ventricular myocytes culture and transfection. Neonatal rat ventricular cardiomyocyte (NRVCs) from 1 to 3-day-old SD rats were isolated and cultured as described previously^{10,11}. Briefly, the hearts were aseptically removed and ventricle tissues were minced and digested in 0.25% trypsin solution. Dispersed cells were suspended in DMEM (HyClone, Logan, UT) containing 10% fetal bovine serum and centrifuged at 1000 rpm for 5 min and resuspended in medium for 2 h. The isolated cells were plated into culture flasks (noncoated) and 0.1 mmol/l bromodeoxyuridine was added into the medium to deplete nonmyocytes. Cardiomyocytes were cultured at 37°C with 5% CO_2 and 95% air. MiR-98-mimic, miR-98 inhibitor and NC were synthesized by Guangzhou RiboBio (Guangzhou, China). Cardiomyocytes were starved in serum-free medium for 24 hours, and then transiently transfected with miR-98 mimic (50 nM), miR-98 inhibitor (100 nM) and NC (50 nM), using X-treme GENE siRNA transfection reagent (Roche, Penzberg Germany) according to the manufacturer's instructions. Forty-eight hours after transfection, neonatal rat ventricular myocytes were subsequently treated with $100 \mu\text{M}$ hydrogen peroxide (H_2O_2) for 4 h.

RNA extraction and Real-time PCR. Total RNA was extracted from cultured NRVCs after different treatments or heart tissues using Trizol reagent (Invitrogen, USA) according to manufacturer's protocols. The levels of miR-98, caspase-3 and Fas mRNA were determined using SYBR Green incorporation on Roche Light-Cycler 480 Real Time PCR system (Roche, Germany), with U6 as an internal control for miR-98 and GAPDH for caspase-3 and Fas. The sequences of primers used were listed as follows: miR-98 F: 5'-GCTGAGGTAGTAAGTTGTATTG-3'; R: 5'-CAGTGCCTGTCGTGGAGT-3'; U6 F: 5'-GCTTCGGCACATATACTAAAAT-3'; R: 5'-CGCTTCACGAATTTGCGTGTGCAT-3'; Fas (mouse) F: 5'-TGCTCAGAAGGATTATATCAAGGAG-3' and R: 5'-CGGGATGTATTACTCAAGCTAAGA-3'; Fas (rat) F: 5'-TGACTGCTACTGTGGAGAAGAC-3' and R: 5'-TCATCGCTGAACGCTACTGG-3'; Caspase-3 (mouse) F: 5'-CTCGTCTGGTACGGATGTG-3' and R: 5'-TCCCATAAATGACCCTTCATCA-3'; Caspase-3 (rat): F: 5'-ATGTCGATGCAGCTAACC-3' and R: 5'-GTCTCAATACCGCAGTCC-3'. GAPDH (mouse) F: 5'-AAGAAGGTGGTGAAGCAGGC-3' and R: 5'-TCCACCACCCAGTTGCTGTA-3'; GAPDH (rat): F: 5'-GGAAAGCTGTGGCGTGAT-3'; R: 5'-AAGGTGGAAG AATGGGAGTT-3'. Quantitative real-time PCR was performed in $20 \mu\text{L}$ volumes with SYBR Green PCR Master Mix (Roche, USA) at 95°C for 10 min and 40 cycles at 95°C for 15 s, 60°C for 30 s and 72°C for 30 s, using Light Cycler 480 (Roche, USA). The amount of target ($2^{-\Delta\Delta\text{CT}}$) was obtained by normalizing to endogenous reference and relative to a calibrator (average of the control samples).

MTT Assay. Cell viability was assessed using MTT (3-[4, 5-dimethylthiazol-2-yl]-2, 5 diphenyl tetrazolium bromide) assay. Briefly, cells were treated as described above (transfection and H_2O_2 treatment, etc.) for indicated time. Next, $20 \mu\text{L}$ of MTT (0.5 mg/ml) was added into each well for an incubation of 4 h. The supernate was discarded, followed by the addition of $150 \mu\text{L}$ of DMSO (dimethyl sulfoxide) into each well with rotation for 10 min to dissolve the formazan. The absorbance was measured at 490 nm using an Infinite M200 microplate reader (Tecan, Salzburg, Austria).

TUNEL staining. The TdT-mediated dUTP nick end labeling (TUNEL) staining was employed to detect the apoptosis in NRVCs and left ventricles (border zones) using a TUNEL fluorescence FITC kit (Roche, USA) according to the manufacturer's instruction. After TUNEL staining, the cardiomyocytes or the ventricular specimens were immersed into DAPI (1:30, Beyotime Biotechnology, China) solution to stain nuclei. Fluorescence staining was viewed by a Laser Scanning Confocal Microscope (FV1000, Olympus, Japan). The apoptotic rate was calculated as TUNEL-positive cells per field.

Annexin V-FITC/propidium iodide (AV/PI) dual staining. The Annexin V-FITC/propidium iodide (AV/PI) Apoptosis Detection kit (Vazyme, Nanjing, China) was also used to examine early apoptosis (Annexin V-FITC+/PI−, Q4), late apoptosis (Annexin V-FITC+/PI+, Q2), and necrosis (Annexin V-FITC−/PI+, Q1) according to the manufacturer's instructions (Vazyme, Nanjing, China). To perform the AV/PI staining procedure, as we described previously, cells were digested with 0.25% trypsin, washed, dual-stained with AV and PI, and then analyzed by flow cytometry (BD Bioscience, USA).

Western Blot Analysis. Total protein was extracted from the NRVCs or peri-infarct region of left ventricular myocardium using RIPA buffer (Sigma-Aldrich, St. Louis, MO, USA) with rotation on ice for 1 h lysis. Subsequently, proteins were separated by electrophoresis on SDS-PAGE (10% polyacrylamide gels) and transferred to nitrocellulose membrane. Next, nitrocellulose membranes were blocked in 5% nonfat milk PBS for 2 hours and then incubated overnight at 4 °C with anti-Fas (1:1000, Abcam, USA), anti-Caspase-3 (1:1000, Cell Signaling Technology, USA), anti-Bcl-2 (1:1000, Cell Signaling Technology, USA), anti-Bax (1:1000, Proteintech, USA) or β -actin (1:1000, ZSGB-Bio, China) primary antibodies, followed by incubation with IRDye secondary antibodies (LI-COR) for 1 hour. The images were captured by the Odyssey CLx Infrared Imaging System (LI-COR Biosciences, Lincoln, NE, USA). Western blot bands were quantified by measuring the intensity in each group using Odyssey CLx version 2.1. The data was normalized to β -actin as an internal control.

Luciferase reporter assay. The rat Fas 3'-UTR (GenBank ID: NM_139194.2, nt 961–1141) was cloned into the multiple cloning site of the pmirGLO dual-luciferase miRNA target expression vector (Promega, Madison, WI, USA), referred to as pmirGLO-Fas. Then, HEK293T cells were seeded in a 96-well plate and co-transfected with 0.5 μ g plasmid and miR-98 mimics or negative controls using Lipofectamine 2000 reagent. Renilla luciferase was used as an internal control. Forty-eight hours after transfection, the cells were collected, and firefly and Renilla luciferase activities were evaluated using Dual-Luciferase Reporter Assay System (Promega, Madison, WI, USA).

Caspase-3 and LDH activity assay. Myocardial caspase-3 activity and serum LDH activity were determined by colorimetric assay kits (Beyotime Institute of Biotechnology, Jiangsu, China; Nanjing Jiancheng Bioengineering Institute, Nanjing, China) as described in our previous study¹¹. The heart tissue and blood samples were collected from mice 3 days after MI and the activity of Caspase-3 and LDH were measured with the colorimetric method according to the manufacturer's protocols, respectively.

Statistical analysis. All data were presented as mean \pm SEM and analyzed by SigmaPlot and SigmaStat Software (Jandel Scientific, CA, USA). Paired t test or Student's t test was used where appropriate. A two-tailed $P < 0.05$ was considered to be statistically significant.

References

1. Thom, T. *et al.* Heart disease and stroke statistics—2006 update: a report from the American Heart Association Statistics Committee and Stroke Statistics Subcommittee. *Circulation*. **113**, e85–151 (2006).
2. Chiong, M. *et al.* Cardiomyocyte death: mechanisms and translational implications. *Cell Death Dis.* **2**, e244 (2011).
3. Nabel, E. G. & Braunwald, E. A tale of coronary artery disease and myocardial infarction. *N Engl J Med.* **366**, 54–63 (2012).
4. Palojoki, E. *et al.* Cardiomyocyte apoptosis and ventricular remodeling after myocardial infarction in rats. *Am J Physiol Heart Circ Physiol.* **280**, H2726–2731 (2001).
5. Bartel, D. P. *et al.* MicroRNAs: genomics, biogenesis, mechanism, and function. *Cell.* **116**, 281–297 (2004).
6. Sala, V. *et al.* MicroRNAs in myocardial ischemia: identifying new targets and tools for treating heart disease. New frontiers for miRNA medicine. *Cell Mol Life Sci.* **71**, 1439–1452 (2014).
7. Goretti, E., Wagner, D. R. & Devaux, Y. miRNAs as biomarkers of myocardial infarction: a step forward towards personalized medicine? *Trends Mol Med.* **20**, 716–725 (2014).
8. Zhu, H. & Fan, G. C. Role of microRNAs in the reperfused myocardium towards post-infarct remodeling. *Cardiovasc Res.* **94**, 284–292 (2012).
9. Li, X. *et al.* Inhibition of microRNA-497 ameliorates anoxia/reoxygenation injury in cardiomyocytes by suppressing cell apoptosis and enhancing autophagy. *Oncotarget.* **6**, 18829–18844 (2015).
10. Hang, P., Sun, C., Guo, J., Zhao, J. & Du, Z. BDNF mediates Down-regulation of MicroRNA-195 Inhibits Ischemic Cardiac Apoptosis in Rats. *Int J Biol Sci.* **12**, 979–989 (2016).
11. Huang, W. *et al.* Combination of microRNA-21 and microRNA-146a Attenuates Cardiac Dysfunction and Apoptosis During Acute Myocardial Infarction in Mice. *Mol Ther Nucleic Acids.* **5**, e296 (2016).
12. Rougvie, A. E. Control of developmental timing in animals. *Nat Rev Genet.* **2**, 690–701 (2001).
13. Su, J., Chen, P., Johansson, G. & Kuo, M. L. Function and regulation of let-7 family microRNAs. *Microrna.* **1**, 34–39 (2012).
14. Yuan, Y. *et al.* MicroRNA-98 and microRNA-214 post-transcriptionally regulate enhancer of zeste homolog 2 and inhibit migration and invasion in human esophageal squamous cell carcinoma. *Mol Cancer.* **11**, 51 (2012).
15. Zhang, B., Pan, X., Cobb, G. P. & Anderson, T. A. microRNAs as oncogenes and tumor suppressors. *Dev Biol.* **1**, 1–12 (2007).
16. Wang, J. *et al.* Screening plasma miRNAs as biomarkers for renal ischemia-reperfusion injury in rats. *Med Sci Monit.* **20**, 283–289 (2014).
17. Li, H. *et al.* miR-98 protects endothelial cells against hypoxia/reoxygenation induced-apoptosis by targeting caspase-3. *Biochem Biophys Res Commun.* **467**, 595–601 (2015).
18. Wang, S. *et al.* Let-7/miR-98 regulate Fas and Fas-mediated apoptosis. *Genes Immun.* **12**, 149–154 (2011).
19. Abbate, A., Bussani, R., Amin, M. S., Vetrovec, G. W. & Baldi, A. Acute myocardial infarction and heart failure: Role of apoptosis. *Int J Biochem Cell Biol.* **38**, 1834–1840 (2006).

20. Shah, A. M. & Mann, D. L. In search of new therapeutic targets and strategies for heart failure: Recent advances in basic science. *Lancet*. **378**, 704–712 (2011).
21. Yang, Y., Ago, T., Zhai, P., Abdellatif, M. & Sadoshima, J. Thioredoxin 1 negatively regulates angiotensin II-induced cardiac hypertrophy through upregulation of miR-98/let-7. *Circ Res*. **108**, 305–313 (2011).
22. Kim, M. J. *et al.* Protection from apoptotic cell death by cilostazol, phosphodiesterase type III inhibitor, via cAMP-dependent protein kinase activation. *Pharmacol Res*. **54**, 261–267 (2006).
23. Zhang, L. *et al.* High-dose glucose-insulin-potassium treatment reduces myocardial apoptosis in patients with acute myocardial infarction. *Eur J Clin Invest*. **35**, 164–170 (2005).
24. Vafaiyan, Z., Gharaei, R. & Asadi, J. The correlation between telomerase activity and Bax/Bcl-2 ratio in valproic acid-treated MCF-7 breast cancer cell line. *Iran J Basic Med Sci*. **18**, 700–704 (2015).
25. Kang, S. *et al.* Myocardium and microvessel endothelium apoptosis at day 7 following reperfused acute myocardial infarction. *Microvasc Res*. **79**, 70–79 (2010).
26. Sun, H. *et al.* Ischemic postconditioning inhibits apoptosis after acute myocardial infarction in pigs. *Heart Surg Forum*. **13**, E305–310 (2010).
27. Chang, J. *et al.* High admission glucose levels increase Fas apoptosis and mortality in patients with acute ST-elevation myocardial infarction: a prospective cohort study. *Cardiovasc Diabetol*. **12**, 171 (2013).
28. Lu, C. *et al.* Toll-like receptor 3 plays a role in myocardial infarction and ischemia/reperfusion injury. *Biochim Biophys Acta*. **1842**, 22–31 (2014).
29. Abbate, A., Biondi-Zoccai, G. G. & Baldi, A. Pathophysiologic role of myocardial apoptosis in post-infarction left ventricular remodeling. *J Cell Physiol*. **193**, 145–153 (2002).
30. Garcia, S. & Conde, C. The role of poly(ADP-ribose) polymerase-1 in rheumatoid arthritis. *Mediators Inflamm*. **2015**, 837250 (2015).
31. Porter, A. G. & Janicke, R. U. Emerging roles of caspase-3 in apoptosis. *Cell Death Differ*. **6**, 99–104 (1999).
32. Zhang, J. *et al.* MicroRNA-25 Negatively Regulates Cerebral Ischemia/Reperfusion Injury-Induced Cell Apoptosis Through Fas/FasL Pathway. *J Mol Neurosci*. **58**, 507–516 (2016).
33. Pan, Z. *et al.* miR-1 exacerbates cardiac ischemia-reperfusion injury in mouse models. *PLoS One*. **7**, e50515 (2012).

Acknowledgements

This work was supported in part by Major Program of National Natural Science Foundation of China (81230081).

Author Contributions

Z.D., C.S. and H.L. wrote the manuscripts and conceived of the study. C.S., J.G., Y.Y., D.Y. and F.H. performed all experiment. Z.D. and H.L. performed the statistical analyses. All co-authors participated in discussion.

Additional Information

Supplementary information accompanies this paper at doi:[10.1038/s41598-017-07578-x](https://doi.org/10.1038/s41598-017-07578-x)

Competing Interests: The authors declare that they have no competing interests.

Publisher's note: Springer Nature remains neutral with regard to jurisdictional claims in published maps and institutional affiliations.



Open Access This article is licensed under a Creative Commons Attribution 4.0 International License, which permits use, sharing, adaptation, distribution and reproduction in any medium or format, as long as you give appropriate credit to the original author(s) and the source, provide a link to the Creative Commons license, and indicate if changes were made. The images or other third party material in this article are included in the article's Creative Commons license, unless indicated otherwise in a credit line to the material. If material is not included in the article's Creative Commons license and your intended use is not permitted by statutory regulation or exceeds the permitted use, you will need to obtain permission directly from the copyright holder. To view a copy of this license, visit <http://creativecommons.org/licenses/by/4.0/>.

© The Author(s) 2017